Electronic Supplementary Material

Highly sensitive and fast-response hydrogen sensing of WO_3 nanoparticles via palladium reined spillover effect

Zhengyou Zhu,[#] Xiaxia Xing,[#] Dongliang Feng, Zhenxu Li, Yingying Tian and Dachi Yang*

Tianjin Key Laboratory of Optoelectronic Sensor and Sensing Network Technology and Department of Electronics, College of Electronic Information and Optical Engineering, Nankai University, Tianjin 300350, China.

* E-mail: yangdachi@nankai.edu.cn

[#] These authors (Z. Zhu and X. Xing) contributed equally to this study.

Outline

Experimental details

Synthesis of WO_3-NPs and Pd-NPs@WO_3-NPs

Pristine WO_3-NPs were synthesized by hydrolysis of WCl_6 in ethanol solution and subsequent pyrolysis treatment. Specifically, 0.8 g WCl_6 was firstly added into 160 mL ethanol under continuous sonication for 30 min to obtain a transparent yellow solution. Secondly, the above solution was aged for 48 h at near room temperature (25~30 ^oC, relative humidity of 60~70%). Thirdly, deep blue floccules formed in the beaker, which were subsequently collected by filtration and rinsed with ethanol and distilled water thoroughly, followed by drying at 60 ^oC for 2 h. Finally, WO_3-NPs were obtained by pyrolysis treatment to the blue powder via heating at 600 ^oC for 2 h in a muffle furnace (KSL1100X, Hefei Kejing Materials Technology Co. Ltd, China).

For the photochemical synthesis of Pd-NPs@WO_3-NPs, 50 mg as-prepared WO_3-NPs (powder) was dispersed in a mixture containing 80 mL deionized (D. I.) water and 20 mL methanol by sonication. Afterward, various volume (0.05, 0.1, 0.5, 1, 2, and 3 mL) of $PdCl_2$ (5 mM, dissolved by HCl assistance) aqueous solution was added, which was then UV-irradiated with irradiation distance of ~ 5 cm under stirring for 120 s by a Xenon light source (CEL-HXUV300, Beijing Zhongjiao Jinyuan Technology Co., Ltd). Finally, the precipitate was separated by filtrating and rinsing in D. I. water, followed by drying at 60 ^oC for 1 h. According to the feeding of $PdCl_2$ precursor, the Pd^{2+} concentrations were 2.5, 5, 25, 50, 100, 150 μM, respectively.

Characterizations

The samples of sensing materials were characterized using field emission scanning electron microscopy (FE-SEM, JEOL-6701F, at 2kV), transmission electron microscopy (TEM, JEM-2200FS) with high-resolution TEM (HRTEM) and selective area electron diffraction (SEAD) patterns, X-ray diffraction (XRD, Rigaku Smart Lab 3 kW) with Cu Kα radiation (2.2 kW) and X-ray photoelectron spectroscopy (XPS, Thermo Scientific ESCALAB 250Xi).

Hydrogen sensing measurements

As-prepared samples were mixed with terpilenol to make a uniform paste. The paste was then coated

on a ceramic tube printed with a pair of Au electrodes, followed by drying at 60 °C in an oven for 2 h. A Ni-Cr alloy wire was inserted into the tube to tune the working temperature. Hydrogen sensing test was carried out employing a static testing device (WS-30B system, Weisheng Instruments Co., Zhengzhou, China). The response of hydrogen is calculated by $S = R_g/R_a$, where R_g and R_a are the resistances in the target gas and air atmosphere, respectively. The response or recovery time is counted as the time taken by the sensor to reach 90% of the saturation signal after hydrogen in or hydrogen off. The ambient temperature and relative humidity during the test were 27 °C and ~70%, respectively. Prior to the test at 50 °C, the sensor was heated at 200 °C for 10 min cycling test to get activated.

Capacitance-voltage (C-V) test

Capacitance-voltage (C-V) test was carried out on the electrode/electrolyte at an electrochemistry workstation (VersaSTAT 4, AMETEK Princeton) to understand the Schottky contacts based on the Mott-Schottky equation, [1, 2]

$$\frac{1}{C^2} = \frac{2}{N_D e \varepsilon_0 \varepsilon}\left(E - E_{FB} - \frac{kT}{e}\right)$$

where C is the space charge capacitance, N_D represents the carrier density, e is the elemental charge, ε_0 and ε are respectively denoted as the permittivity of the vacuum and the semiconductor, E is the applied potential, E_{FB} is the flat band potential, T is the temperature and k is the Boltzmann constant.

Theoretical modulation

Density functional theory (DFT) calculation was performed by using the CP2K package. [3] PBE functional [4] with Grimme D3 correction [5] was used to describe the system. Unrestricted Kohn-Sham DFT has been used as the electronic structure method in the framework of the Gaussian and plane waves method. [6, 7] The Goedecker-Teter-Hutter (GTH) pseudopotentials, [8, 9] DZVPMOLOPT-GTH basis sets [6] were utilized to describe the molecules. A plane-wave energy cut-off of 500 Ry has been employed. We used a unit cell of (4×4) with four atomic layers of WO_3 to model the surface. The Pd-NPs@WO_3-NPs is modeled with Pd10 clusters on the WO_3 surface. All the simulations were

carried out by keeping the two bottom WO_3 layers fixed at the initial coordinates in order to maintain the bulk behavior of the inner part of the slab. The adsorption energy is defined as $E_{ad} = E_{mol/sur} - E_{mol} - E_{sur}$, where E_{ad} is adsorption energy and $E_{mol/sur}$ is total energy for molecule on surface. E_{mol} and E_{sur} are the energy of isolated molecule and surface, respectively.

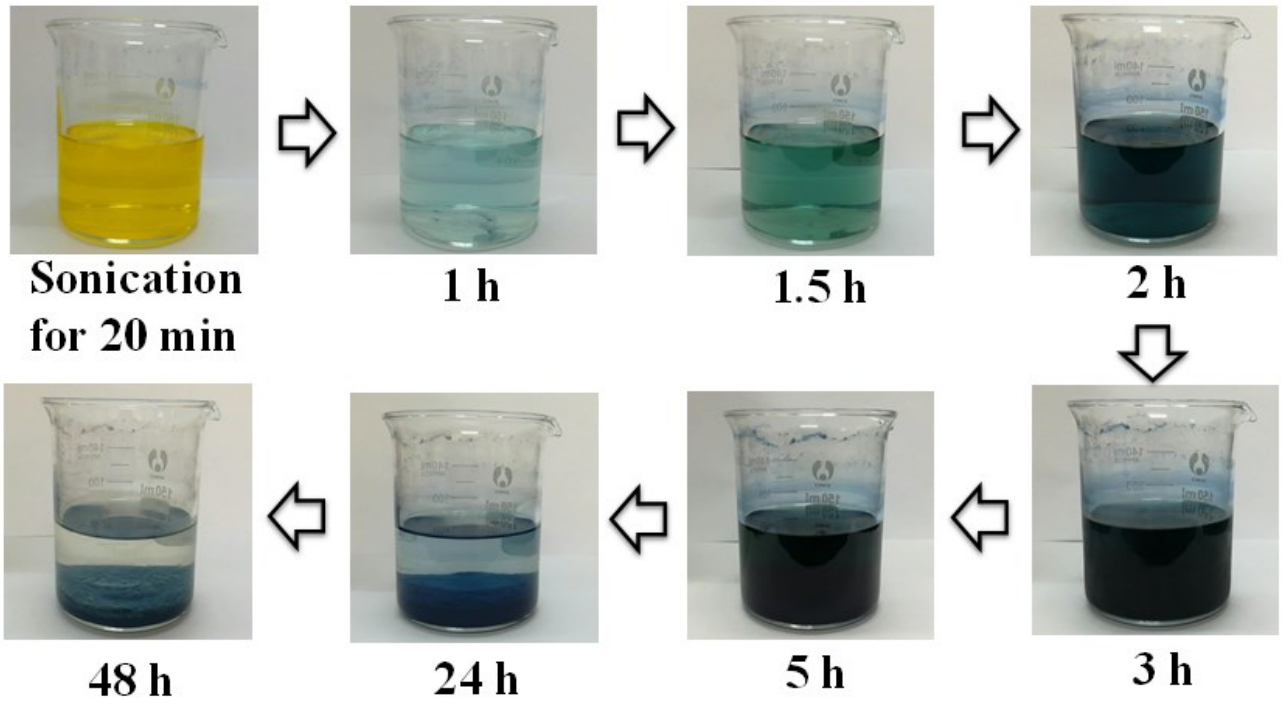

Fig. S1. Color transitions of the reactant during the hydrolysis of WCl_6 in ethanol solution at room temperature.

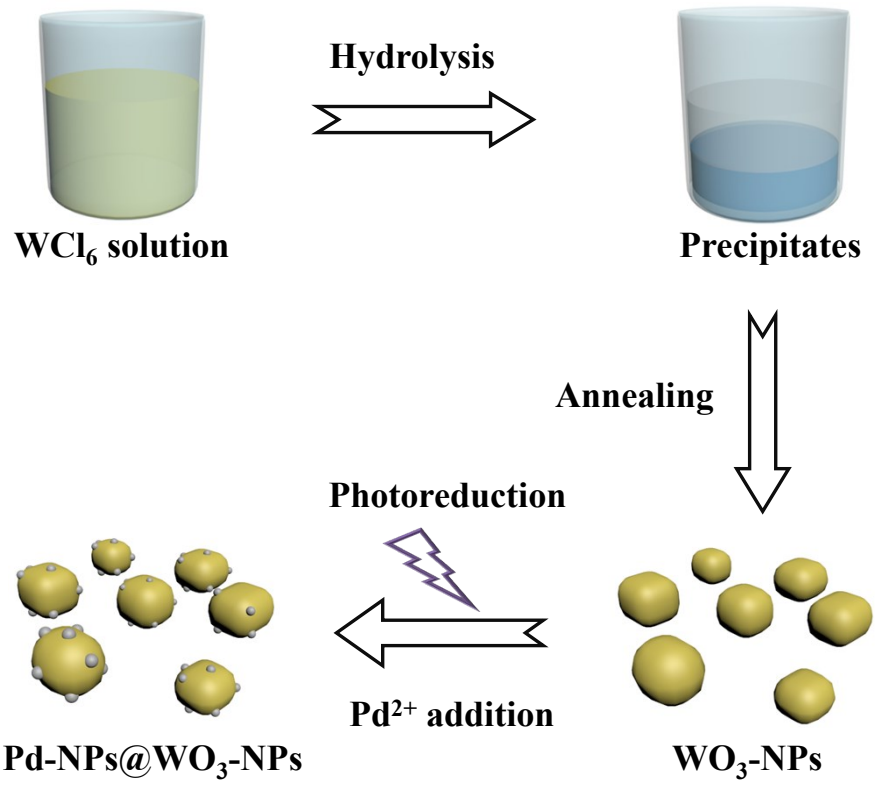

Fig. S2. Synthetic scheme of Pd-NPs@WO_3-NPs via combined hydrolysis, annealing and photochemical deposition.

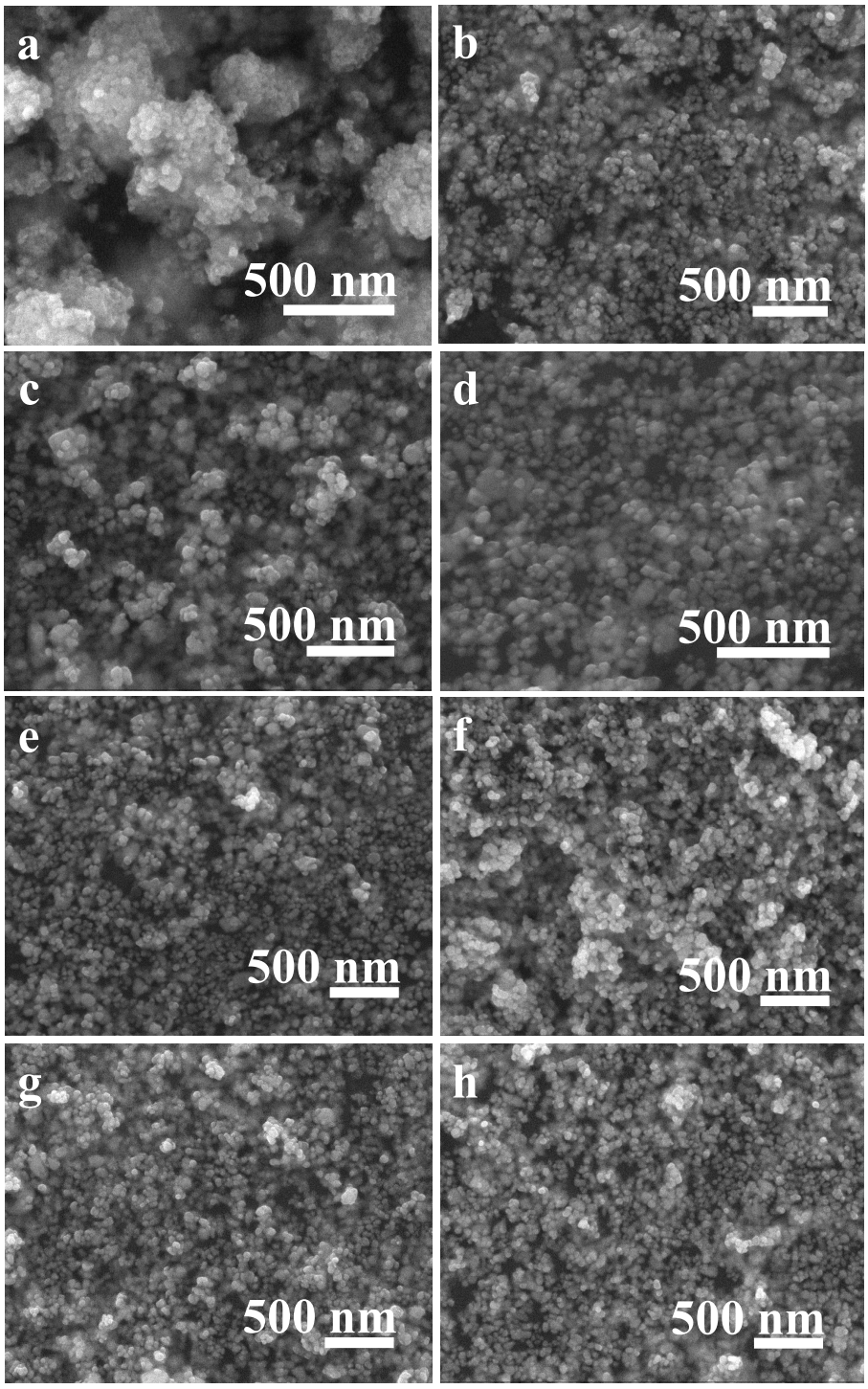

Fig. S3. The SEM images of the (a) precursor prior to annealing, (b) pristine WO_3-NPs, and Pd-NPs@WO_3-NPs containing various concentrations of Pd^{2+} in the precursors of (c) 2.5, (d) 5, (e) 25, (f) 50, (g) 100, (h) 150 μM.

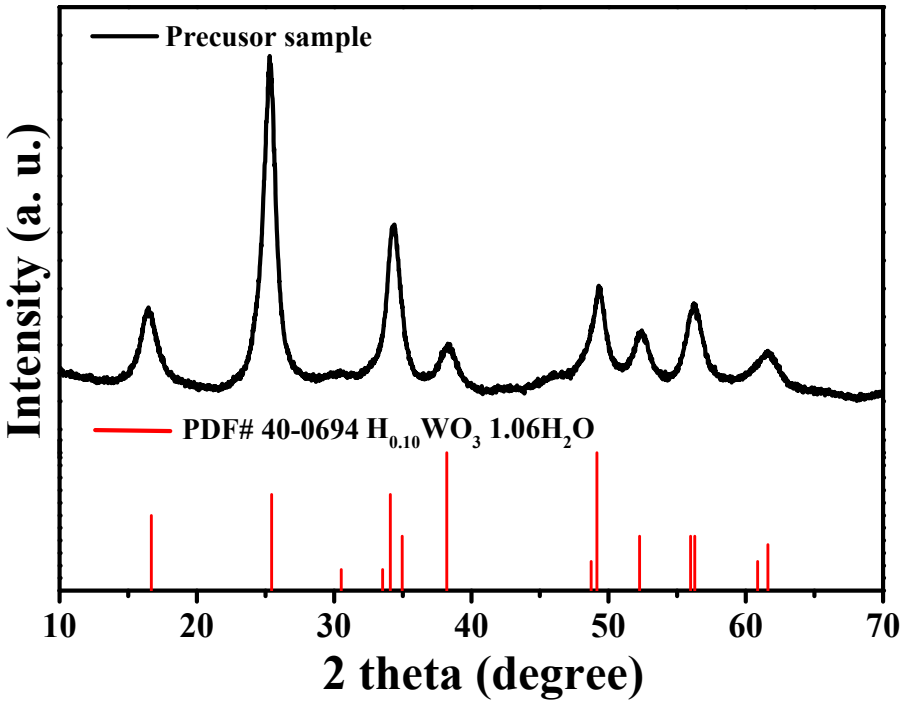

Fig. S4. XRD pattern of the hydrolysis product without annealing.

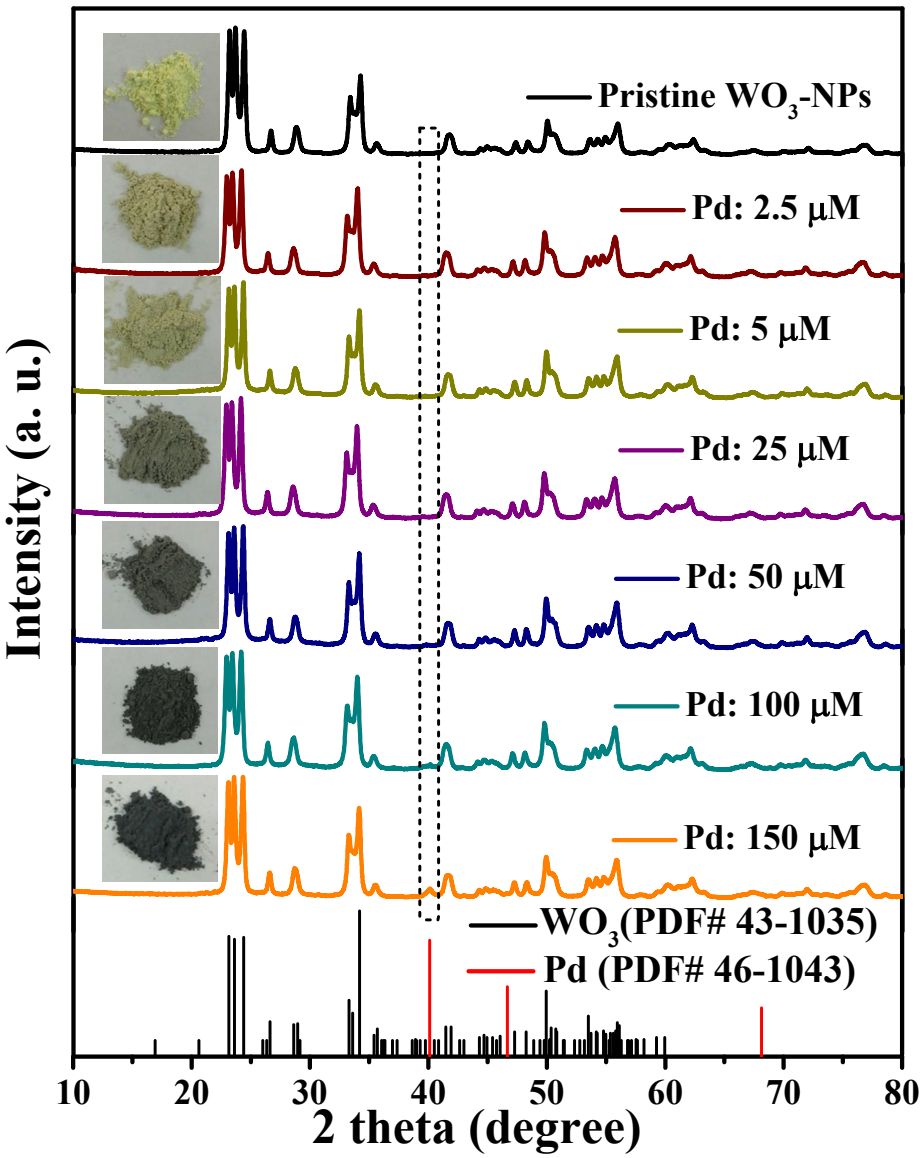

Fig. S5. XRD patterns and the corresponding photos of pristine WO_3-NPs and those containing with applied various concentrations of Pd^{2+} in the precursors.

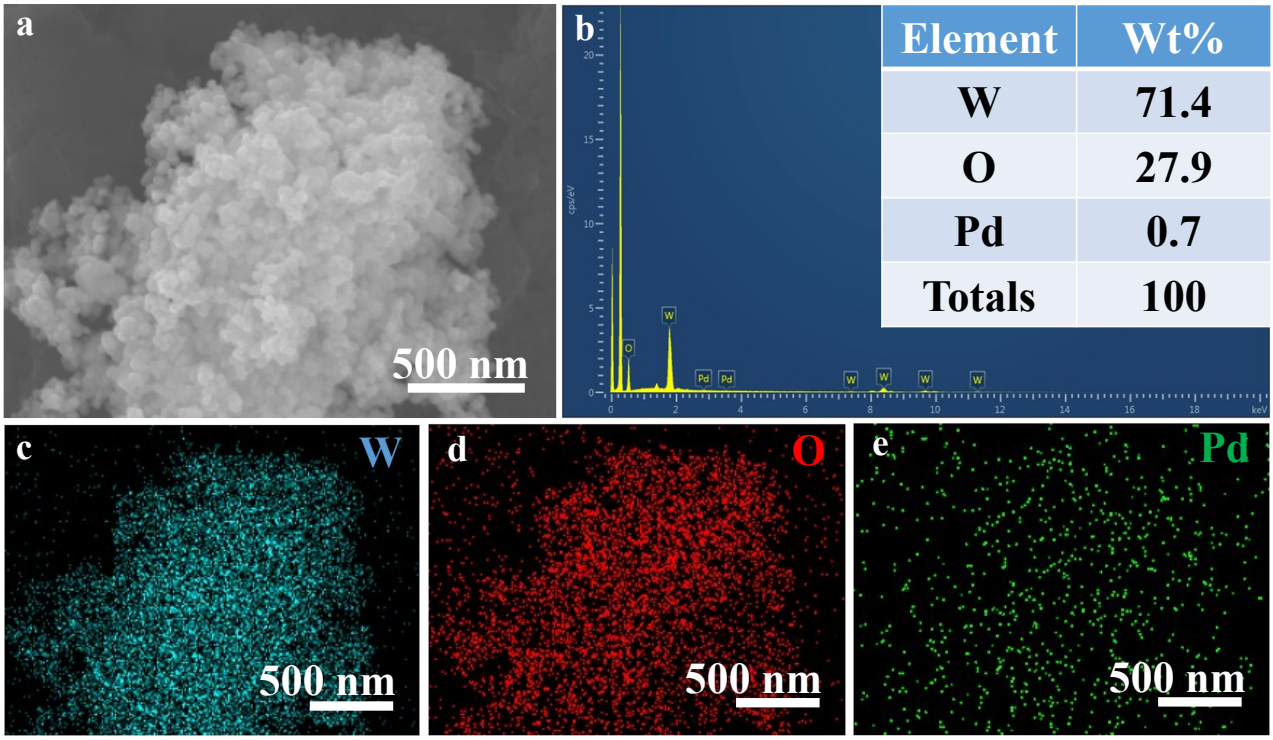

Fig.S6 The EDS elemental mapping of Pd-NPs@WO_3-NPs with applied 25 μM Pd^{2+} in the precursors.

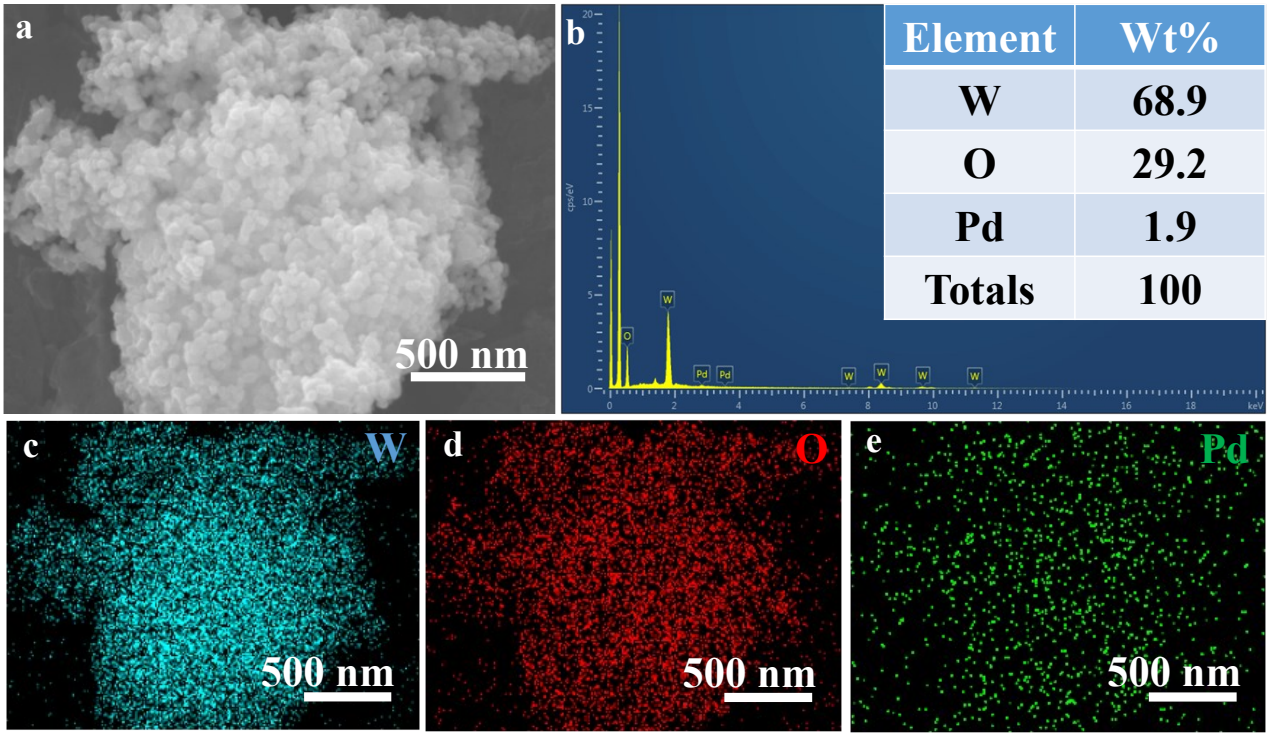

Fig. S7. The EDS elemental mapping of Pd-NPs@WO_3-NPs with applied 100 μM Pd^{2+} in the precursors.

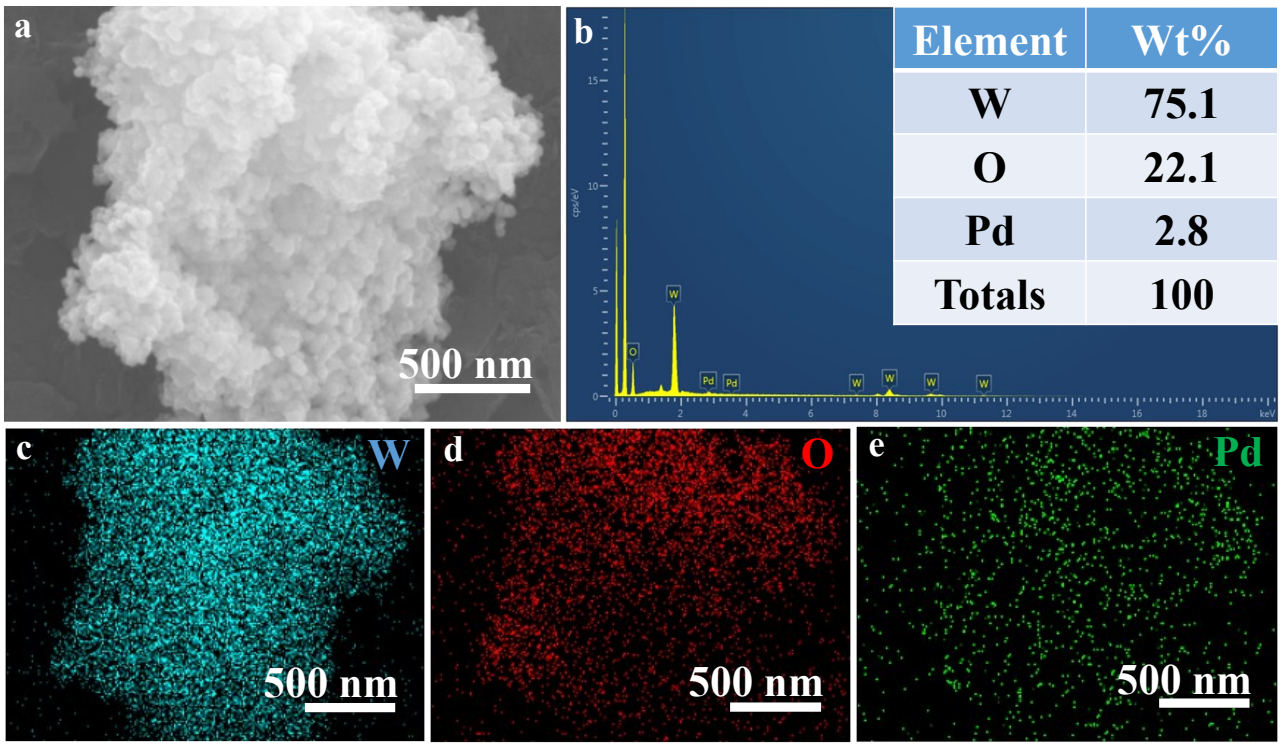

Fig. S8. The EDS elemental mapping of Pd-NPs@WO_3-NPs with applied 150 μM Pd^{2+} in the precursors.

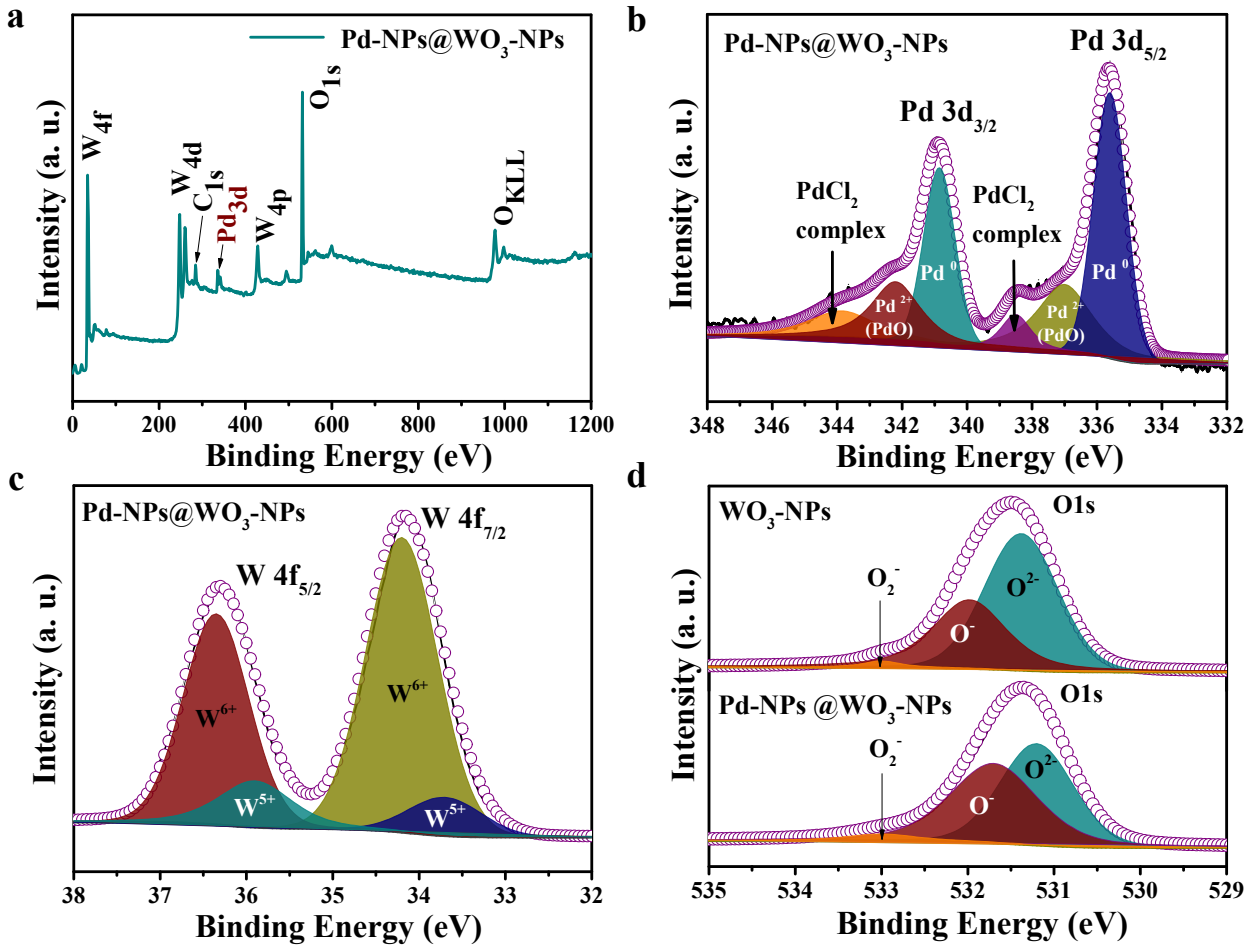

Fig. S9. (a) Survey scan XPS spectrum, (b) Pd 3d spectrum, (c) W 4f spectrum of Pd-NPs@WO_3-NPs, and (d) O 1s spectra of Pd-NPs@WO_3-NPs (Bottom-panel) with pristine WO_3-NPs (Top-panel) for comparison.

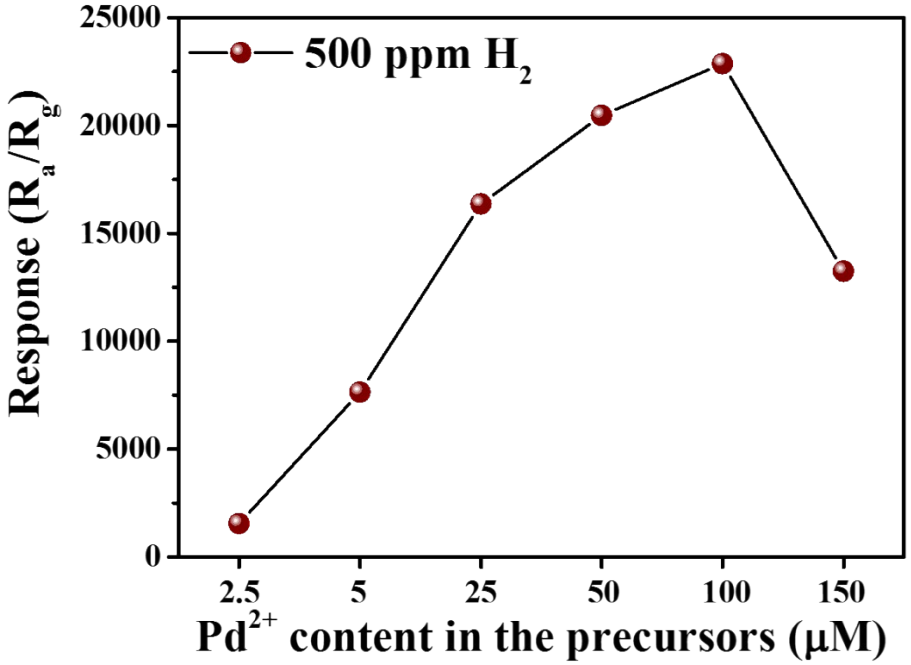

Fig. S10. Hydrogen response of the Pd-NPs@WO_3-NPs sensor to 500 ppm hydrogen with applied various concentrations of Pd^{2+} in the precursors.

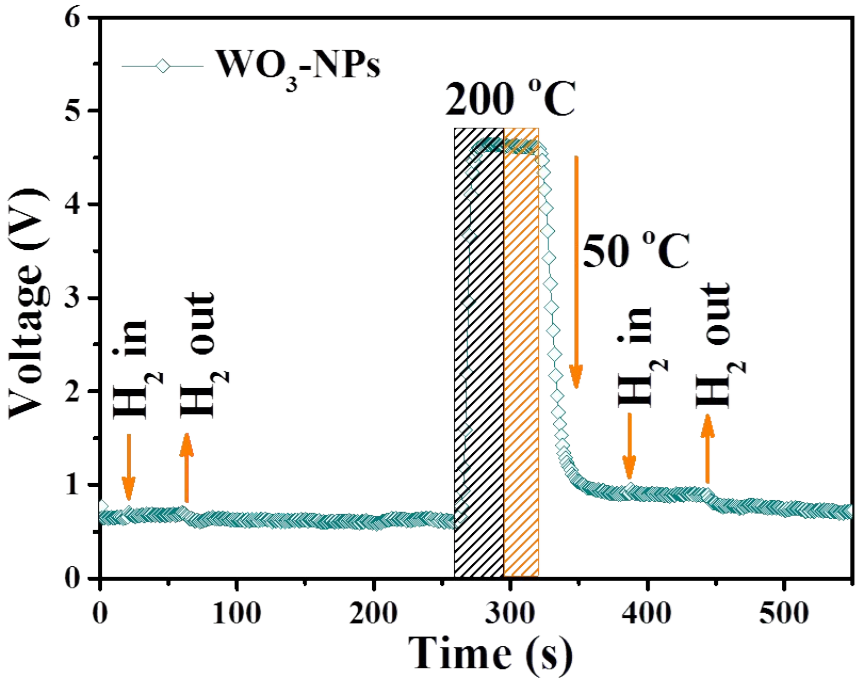

Fig. S11. Response / recovery curve of WO_3-NPs after ageing process.

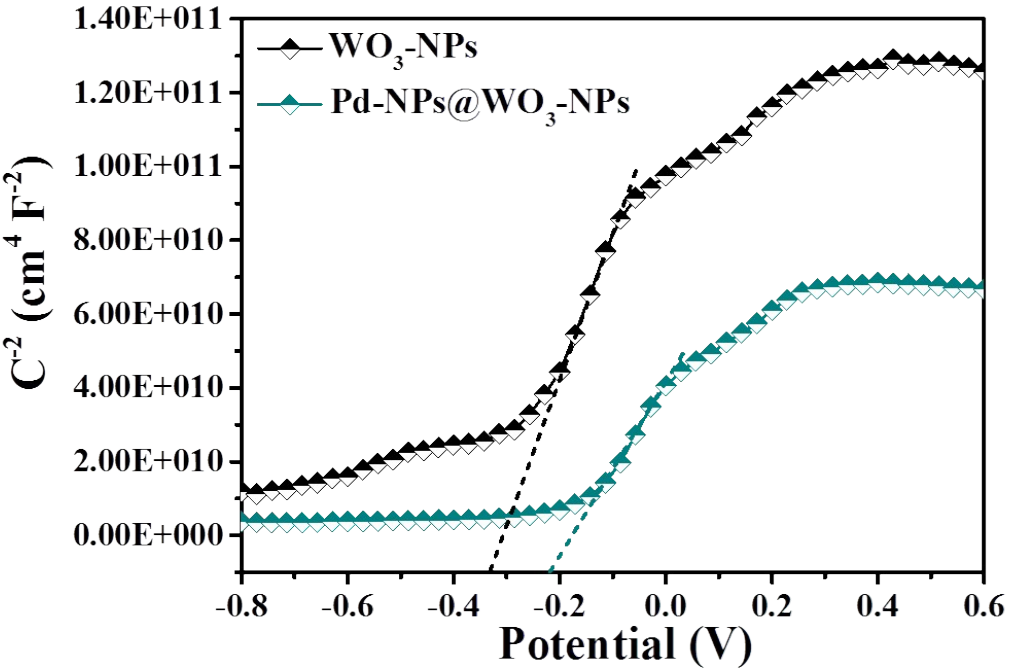

Fig. S12. Mott-Schottky plots of WO_3-NP and Pd-NPs@WO_3-NPs.

Table S1 Comparison of various hydrogen sensors based on precious metal decorated metal oxides.

Materials/ Structures	Operating Temperature (°C)	Hydrogen response @concentration	Detection limit	Response/Recovery Time	Refs.
Pt-In_2O_3 nanocube	Room Temperature	~20 @1.5 vol%	0.5 vol%	33 s/ 66 s@ 1.5 vol%	[10]
Au@ZnO nanoparticle	300	103.9@100 ppm	0.5 ppm	75 s/ 600 s @100 ppm	[11]
Pt-SnO_2 nanowire	100	118@1000ppm	100 ppm	-/-	[12]
Pd-SnO_2 film	300	28@250 ppm	25 ppm	3 s/ 50 s@250 ppm	[13]
Pd-SnO_2 nanowires	400	5.51@100 ppm	10 ppm	35 s/ 30 s@100 ppm	[14]
Pt-WO_3 nanorod	200	~1600@150 ppm	100	~5.5 min/ ~15 min @ 3000 ppm	[15]
Pd-3DOM WO_3	130	382@50 ppm	5 ppm	10 s/ 50 s @50 ppm	[16]
Pd-WO_3 nanoplates	Room Temperature	34@ 0.1 vol%	0.05 vol%	54 s/ - @0.05 vol%	[17]
Pd-WO_3 nanotubes	450	17.6@500 ppm	5 ppm	25 s/- @500 ppm	[18]
Pd-WO_3 nanoplates	80	169.3@0.1 vol%	0.1 vol%	42.8 s/ 48.5 s@0.1 vol%	[19]
Pd-NPs@WO_3-NPs	~50	22867@500 ppm	5 ppm	1.2 s/ 5~99 s @500 ppm	This study

Table S2 The H_2 and O_2 adsorption energy of the DFT calcluation and comparison.

	O_2 adsorption energy (E_{ad}) / eV	**H_2 adsorption energy (E_{ad}) / eV**
WO_3-NPs	-1.05	-2.8
Pd-NPs@WO_3-NPs	-1.86	-0.53

References

1. Z. Zhang, Y. Yu and P. Wang, *ACS Appl. Mater. Interfaces*, 2012, **4**, 990-996.
2. M. Ye, J. Gong, Y. Lai, C. Lin and Z. Lin, *J. Am. Chem. Soc.*, 2012, **134**, 15720-15723.
3. J. Hutter, M. Iannuzzi, F. Schiffmann and J. Vandevondele, *Wires. Comput. Mol. Sci.*, 2014, **4**, 15-25.
4. Y. Zhang and W. Yang, *Phys. Rev. Lett.*, 1998, **80**, 890-890.
5. S. Grimme, *J. comput. Chem.,* 2006, **27**, 1787-1799.
6. J. VandeVondele and J. Hutter, *J. chem. Phy.*, 2007, **127**, 114105.
7. J. VandeVondele, M. Krack, F. Mohamed, M. Parrinello, T. Chassaing and J. Hutter, *Comput. Phys. Commun.*, 2005, **167**, 103-128.
8. S. Goedecker, M. Teter and J. Hutter, *Phys. Rev. B*, 1996, **54**, 1703.
9. C. Hartwigsen, S. Gœdecker and J. Hutter, *Phys. Rev. B*, 1998, **58**, 3641.
10. Y. Wang, B. Liu, D. Cai, L. Han, L. Yuan, D. Wang, L. Wang, Q. Li and T. Wang, *Sens. Actuators B Chem.*, 2014, **201**, 351-359.
11. S. M. Majhi, P. Rai and Y. T. Yu, *ACS Appl. Mater. Interfaces*, 2015, **7**, 9462-9468.
12. Y. Shen, YAMAZAKI, Toshinari, Z. Liu, D. Meng, KIKUTA and Toshio, *J. Alloy. Compd.*, 2009, **488**, L21-L25.
13. N. V. Toan, N. V. Chien, N. V. Duy, H. S. Hong, H. Nguyen, N. D. Hoa and N. V. Hieu, *J. Hazard. Mater.*, 2016, **301**, 433-442.
14. K. Nguyen, C. M. Hung, T. M. Ngoc, D. T. Thanh Le, D. H. Nguyen, D. Nguyen Van and H. Nguyen Van, *Sens. Actuators B Chem.*, 2017, **253**, 156-163.
15. M. Horprathum, T. Srichaiyaperk, B. Samransuksamer, A. Wisitsoraat, P. Eiamchai, S. Limwichean, C. Chananonnawathorn, K. Aiempanakit, N. Nuntawong and V. Patthanasettakul, *ACS Appl. Mater. Interfaces*, 2014, **6**, 22051-22060.
16. Z. Wang, S. Huang, G. Men, D. Han and F. Gu, *Sens. Actuators B Chem.*, 2018, **262**, 577-587.
17. B. Liu, D. Cai, L. Yuan, D. Wang, L. Wang, Y. Wang, L. Han, Q. Li and T. Wang, *Sens. Actuators B Chem.*, 2014, **193**, 28-34.
18. S. J. Choi, S. Chattopadhyay, J. J. Kim, S. J. Kim, H. L. Tuller, G. C. Rutledge and I. D. Kim, *Nanoscale*, 2015, **8**, 9159.
19. Y. Wang, B. Liu, H. Li, L. Wang, D. Cai, D. Wang, Y. Liu, Q. Li, T. Wang and S. Xiao, *J. Mater. Chem. A*, 2014, **3**, 1317-1324.